Vol. 595: 171–186, 2018
https://doi.org/10.3354/meps12553

MARINE ECOLOGY PROGRESS SERIES
Mar Ecol Prog Ser

Published May 14

Coastal upwelling fronts as a boundary for planktivorous fish distributions

Mei Sato[1,4,*], John A. Barth[1], Kelly J. Benoit-Bird[1,2], Stephen D. Pierce[1], Timothy J. Cowles[1], Richard D. Brodeur[3], William T. Peterson[3]

[1]College of Earth, Ocean, and Atmospheric Sciences, Oregon State University, 104 CEOAS Admin Bldg., Corvallis, OR 97331, USA
[2]Monterey Bay Aquarium Research Institute, 7700 Sandholdt Road, Moss Landing, CA 95039, USA
[3]National Oceanic and Atmospheric Administration, Northwest Fisheries Science Center, Hatfield Marine Science Center, Newport, OR 97365, USA

[4]*Present address:* Institute for the Oceans and Fisheries, The University of British Columbia, AERL Building, 2202 Main Mall, Vancouver, BC V6T1Z4, Canada

ABSTRACT: Fronts have long been considered as bio-aggregators across the food web, serving as important foraging grounds for multiple trophic levels. However, the effect of fronts on intermediate trophic levels is not well understood. We hypothesized that for animals whose metabolic rates are strongly temperature dependent, physiological tolerance will have a more significant impact on their distributions than other biotic factors. We examined this hypothesis through assessment of the spatial variability of planktivorous fish and their dominant zooplankton prey associated with the seasonal and latitudinal variability of the upwelling fronts in the Northern California Current System. Acoustically observed fish biomass dominated by planktivorous species was higher offshore of the upwelling front than inshore. In contrast, zooplankton scattering layers dominated by euphausiids were generally associated with the 200 m isobath, regardless of the position of the front. Fish distributions were consistently found offshore of the upwelling front, aggregating them in the regions of warmer temperature. This suggests that the upwelling front acts as a shoreward boundary for planktivorous fish. With the offshore movement of the upwelling front away from the 200 m isobath as the upwelling season progressed, overlap between planktivorous fish and their zooplankton prey would be decreased. The boundary effect of coastal upwelling fronts on the distributions of mid-trophic level organisms indicates their important role in predator–prey interactions and energy transfer through food webs via a radically different mechanism than previously assumed.

KEY WORDS: Upwelling · Fronts · California Current System · Predator–prey interactions · Acoustics

INTRODUCTION

Biological–physical interactions structure the variability of the ocean at a wide range of spatial and temporal scales, affecting population dynamics and trophic interactions (Haury et al. 1978, Bakun 1996). Physical processes often set the stage on which the biological play is enacted to create the structure of life in the ocean. One such example is at a front, a physical interface with sharp gradients of water properties including temperature, salinity, and/or turbidity (Joyce 1983, Le Fèvre 1987). These fronts occur across the world's oceans, ranging from basin-scale features to small river plumes, and can be persistent or ephemeral (Le Fèvre 1987, Belkin et al. 2009). Frontal zones are often associated with enhanced biomass and may serve as important foraging grounds by aggregating species from multiple tro-

*Corresponding author: m.sato@oceans.ubc.ca

phic levels (Franks 1992a, Genin et al. 2005, Bost et al. 2009), hence being critical habitats for successful energy transfer through food webs.

The conceptual view of fronts as bio-aggregators has been developed largely based on studies focusing on primary and secondary production and top predators. Surface convergence, which is a major characteristic of fronts, retains nutrient-enhanced primary productivity and accumulates phytoplankton (Traganza et al. 1987, Franks 1992a, Yoder et al. 1994). Zooplankton actively swim against the flow caused by fronts, forming aggregations at frontal boundaries (Franks 1992b, Genin et al. 2005). Such convergence zones correspond to aggregations of large predatory fish (Young et al. 2001, Seki et al. 2002), seabirds, and marine mammals (see review by Bost et al. 2009). A missing link in the food webs, however, is the understanding of the mechanisms driving distributions of intermediate trophic levels such as planktivorous fish. Due to the concentrated planktonic food sources and the observation of piscivore aggregations at fronts as well as high abundance of juvenile and larval fishes associated with mesoscale eddies (Logerwell & Smith 2001, Nishimoto & Washburn 2002, Sabarros et al. 2009), it has been assumed that planktivorous fish also aggregate at frontal zones. However, few studies have focused on the relationship between oceanic fronts and planktivorous fish (Lara-Lopez et al. 2012, McClatchie et al. 2012).

Predator–prey interactions are not the sole factor in determining the distribution of animals in the ocean. Temperature is a well documented driver of the distributions of organisms at both large and small scales (Worm et al. 2005, Tittensor et al. 2010). Relationships between physiological optima and limits under different temperatures, oxygen, and other biotic and abiotic factors determine the spatial distributions of fish (Pörtner & Farrell 2008, Sunday et al. 2011, Peck et al. 2013). Growth and reproduction of ectothermic organisms are strongly dependent on temperature, ultimately affecting their population abundance (Pörtner & Knust 2007). Since wind-driven coastal upwelling commonly generates thermal fronts with a strong horizontal temperature contrast (Huyer 1983), these fronts may serve as a physiological boundary and constrain an individual's habitable range. We hypothesize that for animals whose metabolic rates are strongly temperature dependent, including key mid-trophic level animals like planktivorous fish, physiological tolerance may have a more significant impact on their distributions than other biotic factors such as prey availability, potentially resulting in spatial mismatches between these animals and their prey.

We examined spatial variability of planktivorous fish and their dominant zooplankton prey in the Northern California Current System. Our goal was to assess the role of an upwelling front on the distributions of mid-trophic level organisms. By employing ship-based surveys integrating hydrographic, optical, and acoustic measurements, we simultaneously characterized the spatial distributions of multiple trophic levels and their physical environment. We also compared 2 zones of our study area known to have significant difference in upwelling winds (Huyer 1983, Bograd et al. 2009) to examine seasonal shifts in planktivorous fish distributions associated with the upwelling fronts. An understanding of the differential effect of the fronts on organisms across the food web provides a new perspective on how these ecosystems function.

MATERIALS AND METHODS

Study site

In the Northern California Current System (Fig. 1a), upwelling is primarily a summer phenomenon driven by wind along the coast. Topographic features play an important role in the local intensity and spatial extent of upwelling. For example, Heceta Bank off central Oregon deflects the upwelling jet, widening the influence of upwelling and creating an area of retention for nutrient-rich water that leads to increased primary productivity (Barth et al. 2005) and high densities of euphausiids (Ressler et al. 2005). Cape Blanco, whose coastline extends offshore, influences the circulation that separates the upwelling jet and front from the shelfbreak to offshore waters (Barth et al. 2000). There is significant latitudinal variability in southward wind forcing during summer, with increased strength and longer upwelling periods in the southern latitudes (Huyer 1983, Bograd et al. 2009). As a result of these spatio-temporal processes, the timing, location, and intensity of the upwelling front are highly dynamic (Castelao et al. 2005, Venegas et al. 2008).

Survey design

Sampling was designed to include a region between Newport, Oregon (44.6° N), and Crescent City, California (41.9° N; Fig. 1b). Ship-based sampling was conducted by the Northeast Pacific Global Ocean Ecosystem Dynamics (GLOBEC) program (Batchelder et al. 2002) over 2 yr during May–June, to sample

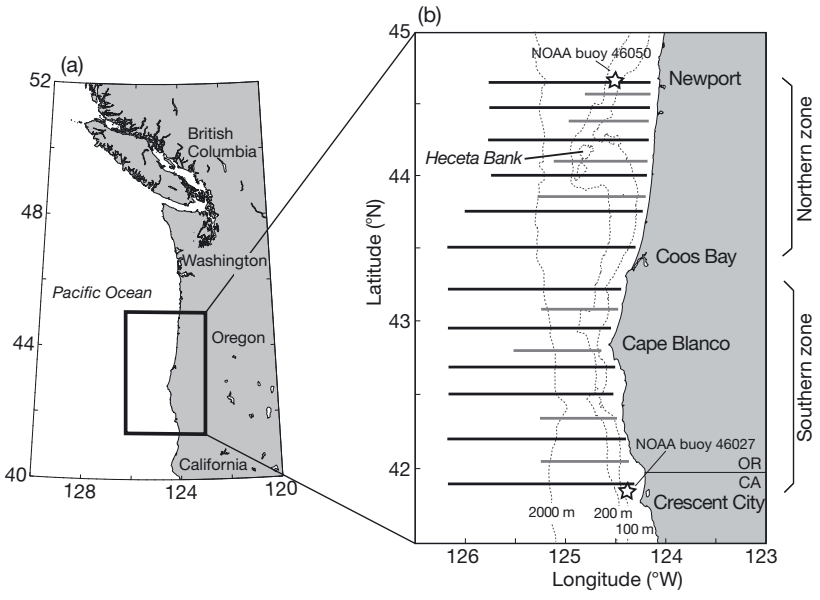

Fig. 1. (a) Study region in the Northeast Pacific. (b) Mesoscale transects (black solid lines) were surveyed by all cruises, while other short transects (gray solid lines) were surveyed by some cruises. Length of the mesoscale transects varied between cruises, depending on the locations of the upwelling fronts. Study region was divided into the northern and southern zones. Winds were measured at the NOAA National Data Buoy Center buoy 46050 located off Newport, Oregon, and 46027 off Crescent City, California. The 100, 200, and 2000 m isobaths are shown as dotted lines

early in the upwelling season, and July–August, to sample fully developed upwelling (Table 1). The study area was divided into the northern and southern zones (Fig. 1b) to examine latitudinal variability of upwelling characteristics at the mesoscale (20–200 km). The boundary between the northern and southern zones was determined to encompass major topographic features at each zone (Heceta Bank and Cape Blanco), associated changes in the upwelling jet, and latitudinal variability in wind forcing. There were 20 parallel, east–west transect lines whose lengths varied between 60 and 160 km depending on the cruises, with repeated surveys on some of the transects (Table 1). The mesoscale transects were separated by ~28 km in the latitudinal direction and covered inshore and offshore of the upwelling fronts; transect lengths were shorter during May–June than during July–August due to the nearshore positioning of the front. Other east–west transects, positioned between mesoscale transects to obtain fine-scale patterns, were surveyed depending on the time available. Ship-based surveys were conducted continuously, resulting in a mixture of daytime and night-time coverage within transects. Simultaneous measurements of biological and physical properties were conducted using concurrently towed, multifrequency echosounders and an undulating vehicle equipped with hydrographic and optical sensors. Typical vessel speed during surveys was approximately 7–8 knots (3.6–4.1 m s^{-1}). Data collected during the northward wind events persisting over 5 d, resulting in downwelling conditions, were excluded from analysis.

Data collection and analysis

Environmental data

Winds were measured at the NOAA National Data Buoy Center buoy 46050 (44.7° N, 124.5° W) located off Newport for the northern zone, and buoy 46027 (41.9° N, 124.4° W) located off Crescent City for the southern zone (Fig. 1b). Wind stress was calculated based on the method of Large & Pond (1981). The hourly data were low-pass filtered to remove diurnal variations. To estimate the cumulative alongshore wind stress during the upwelling seasons, along-

Table 1. Summary of daytime acoustic surveys for fish and zooplankton distributions. Total number of transects: total number of transects covered by the daytime acoustic surveys regardless of their repetitive coverage on the same transects; independent transects: number of transects after removing the repeated surveys on the same transects; NASC: nautical area scattering coefficients

Survey	Date	Ship	Total no. of transects (independent transects)	Total distance surveyed (km)	NASC (mean ± SD; m^2 nmi^{-2}) Fish	Zooplankton
June 2000	30 May– 16 June	RV 'Wecoma'	8 (8)	421.4	235.3 ± 182.2	4.6 ± 24.1
June 2002	1–17 June	RV 'Thomas G. Thompson'	16 (12)	777.9	1343.0 ± 1320.0	32.2 ± 266.9
August 2000	30 July – 17 August	RV 'Wecoma'	24 (17)	1411.6	1302.5 ± 1270.4	64.0 ± 210.3
August 2002	1–19 August	RV 'Roger Revelle'	19 (10)	1260.1	470.9 ± 558.9	34.4 ± 155.7

shore wind stress was summed starting from the spring transition (Huyer et al. 1979, Barth et al. 2005).

Temporal and spatial variability of environmental properties was measured by the towed, undulating vehicle SeaSoar equipped with a conductivity-temperature-depth (CTD) sensor (SBE 911plus; Sea-Bird Electronics) and a fluorometer (FlashPak; WET Labs). Raw variables from the CTD were converted to variables of interest using factory calibrations. The SeaSoar vehicle was towed from a winch, profiling between surface and near bottom or as deep as 110 m. Data were averaged over 1.25 km horizontal by 2 m vertical bins. Using the averaged temperature, salinity, and pressure data, we estimated the geopotential anomaly ($\Delta\Phi$; dynamic height in meters multiplied by the acceleration of gravity) at 5 m relative to 80 m. Geopotential anomaly fields have been used to identify the location of the equatorward upwelling jet because the effect of the upwelling on the strong seasonal pycnocline and the accompanying alongshore coastal jet are observable (Barth et al. 2000). Here, we chose $\Delta\Phi = 1.8$ m^2 s^{-2} as the physical definition of the upwelling front and used it as a reference point to examine fish distributions. Spatial maps of temperature and geopotential anomaly at 5 m depth were constructed using a Barnes objective analysis, where horizontal grid spacing was 0.01°, and the smoothing length scale was 0.5° in latitude (56 km) and 0.3° in longitude (24 km). Spatial maps of chlorophyll *a* concentrations at 5 m depth were constructed using a minimum curvature method in Surfer (Golden Software) with horizontal grid spacing of 0.03° in longitude and latitude. To avoid the effect of temporal changes in mesoscale oceanographic processes and repeated coverage of the same transect lines, we only used the mesoscale transect data collected during both day and night over 4–6 d for the spatial maps.

Acoustic data

Acoustic backscatter data were collected using multifrequency echosounders (Hydroacoustics Technology Inc., Model 244) operated at 38 kHz (7° split beam), 120 kHz (6° split beam), 200 kHz (3° split beam), and 420 kHz (7° single beam). The centers of each transducer were no more than 51 cm apart on the towed body to maximize spatial overlap of the beams. Transducers were deployed on a towed body positioned at approximately 4–12 m depth. Echosounders operated at 0.7–1 ping s^{-1} with a pulse duration of 200 µs. Raw data were automatically averaged into 13 s horizontal (approximately 50 m) and 1 m vertical bins, and the averaged volume backscattering strength (S_v; dB re 1 m^{-1}) using a constant sound speed of 1486 m s^{-1} was recorded. All echosounders were calibrated by the manufacturer before the first cruise of each year in 2000 and 2002.

Pre-processing. Acoustic data were pre-processed using Echoview (version 6.1; Echoview Software). Data shallower than 9 m depth were removed from analyses to eliminate near-field transducer effects and to reduce backscatter from surface bubbles. Near-surface data were visually inspected, and further contaminations due to bubbles below 9 m depth were manually corrected. The echosounder-detected bottom was visually inspected, corrected if necessary, and data within 2 m of the bottom were removed from the analyses. Background noise was removed using a technique developed by De Robertis & Higginbottom (2007) with a minimum signal-to-noise ratio of 6 dB and maximum noise threshold of −125 dB re 1 m^{-1}. Data were smoothed by applying 3 samples × 3 bins (approximately 150 m horizontal × 3 m vertical) running medians to reduce stochastic difference in patterns among frequencies having physical separation of transducers, then exported from Echoview to Matlab (Mathworks, R2013a) for further analysis.

Acoustic classification of dominant taxa. Due to low resolution of the recorded S_v data, we could not explore patches smaller than 50 m in horizontal extent. Therefore, all identified layer structures were greater than 50 m. We examined the acoustic backscatter from both day and night surveys that had no diel vertical migration behavior in the water column. Daytime was defined from 3 h after sunrise through 3 h before sunset, and night-time was defined from 1.5 h after sunset through 1.5 h before sunrise. Sunrise and sunset times at the study site were obtained from the US Naval Observatory (http://aa.usno.navy.mil/data/index.php).

Acoustic backscatter was classified into 2 categories, one attributed to fish with swimbladders and one to zooplankton, based on the observed frequency response (Kang et al. 2002, Sato et al. 2015). In order to identify aggregations within the upper 200 m, we used the 38 and 120 kHz frequencies in calculating the difference in volume backscattering strength ($\Delta S_{v,\, i-j} = S_{v,\, i} - S_{v,\, j}$ where i and j denote frequency in kHz). Cells with $-5.0 \leq \Delta S_{v\ 120\text{-}38\text{kHz}} < 6.5$ dB re 1 m^{-1} were assigned to the 'fish' category, and those with $6.5 \leq \Delta S_{v\ 120\text{-}38\text{kHz}} < 18.5$ dB re 1 m^{-1} were assigned to the 'zooplankton' category (Fig. 2). Using these classifications, all data not classified as 'fish' were masked out in

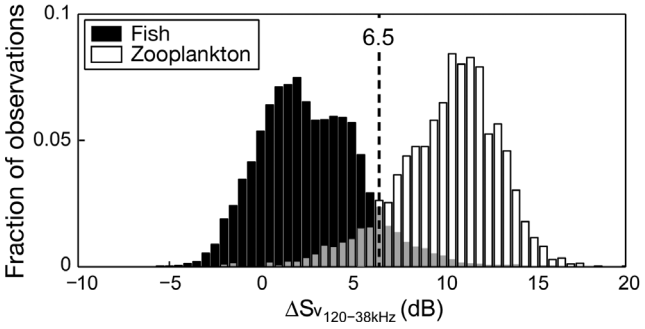

Fig. 2. Histograms of frequency response of 'fish' and 'zooplankton' categories, with the dashed line indicating the value at which the 2 groups were separated based on the difference in volume backscattering strength ($\Delta S_{v\ 120\text{-}38kHz}$). Overlap area between 2 histograms is shown in gray

the 38 kHz echogram, and all data not classified as 'zooplankton' were masked out in the 120 kHz echogram. To examine the effect of the upwelling front on spatial distributions of pelagic organisms, daytime 'fish' in the upper water column (≤100 m depth and shallower than 60 m above the bottom) and daytime 'zooplankton' in the deeper water column (>100 m depth or within 60 m of the bottom) were analyzed (see the Appendix for details).

Net sampling

Fish trawling was conducted mostly during daytime using a Nordic 264 rope trawl (30 m wide × 18 m deep; Nor'Eastern Trawl Systems) from chartered fishing vessels (FV 'Sea Eagle' in 2000, FV 'Frosti' in 2002). A trawl was towed in surface waters for 30 min at a vessel speed of approximately 3 knots (1.7 m s^{-1}). Mesh size of the trawl ranged from 162.6 cm in the body of the net to 8.9 cm in the codend, with a 6.1 m long, 0.8 cm mesh knotless liner sewn into the codend. All pelagic fish were identified to species and counted, and a subsample of each species was measured for fork length (FL) or standard length (SL) depending on fish species. All samples were standardized by the towed area estimated based on the width of the trawl and the towed distance. Additional sampling details are described by Brodeur et al. (2004) and Reese & Brodeur (2006). Spatial overlaps between the daytime trawling stations and high biomass of acoustically observed fish, integrated over 9–20 m to match with approximate trawling depth, occurred during cruises in June 2002 (3 trawls) and August 2000 (6 trawls). The identified trawls were combined for each cruise to examine species composition of potential acoustic backscatterers. There was a temporal mismatch between the trawling and acoustic measurements of 2–27 h. No trawls were conducted near the high biomass regions during June 2000 and August 2002.

Zooplankton were sampled using a Multiple Opening/Closing Net and Environmental Sensing System (MOCNESS; Wiebe et al. 1985) configured with 10 nets (335 µm mesh) with a 1 m^2 mouth opening. Depth-stratified oblique tows were conducted from a vessel (RV 'New Horizon' during June and August 2000 and August 2002, RV 'Wecoma' during June 2002) at a vessel speed of approximately 2.5 knots (1.3 m s^{-1}), closely following the ship conducting the acoustic surveys. Only MOCNESS tows that successfully targeted the daytime zooplankton scattering layers (6 samples) were examined in this study. Those samples were collected within 2 h of the acoustic measurements to minimize spatial and temporal mismatches between net sampling and acoustic measurements. Samples were fixed in 5% formalin in seawater buffered with sodium borate. In the laboratory, a subsample of the net contents was identified to species under a dissecting microscope. Density of abundant taxonomic groups was estimated based on the filtered volume. Additional details are described by Ressler et al. (2005).

Characterizing spatial distributions of planktivorous fish and their zooplankton prey

We examined horizontal distributions of planktivorous fish and zooplankton based on vertically integrated acoustic backscatter. Nautical area scattering coefficient (NASC; m^2 nmi^{-2}), which is a linear measure of integrated backscatter, was calculated in the upper water column for fish and in the deeper water column for zooplankton using a −85 dB re 1 m^{-1} S_v integration threshold. Spatial maps of vertically integrated acoustic backscatter for fish and zooplankton were constructed using a minimum curvature method in Surfer with horizontal grid spacing of 0.03° in longitude and latitude. All mesoscale transects surveyed during the daytime were included in the spatial maps of NASC values, along with other daytime transects that were not part of the mesoscale survey. When there were repeated surveys on the same transect lines, the one with the longer distance was chosen. To examine the effect of the upwelling front on animal distributions, the front ($\Delta\Phi$ = 1.8 m^2 s^{-2}) was identified on the same transects used for the daytime acoustic surveys for fish and zooplankton. When multiple upwelling fronts were detected along a transect, the one closest to the shore was chosen.

Fish distributions relative to the upwelling fronts were examined for each cruise. We used a series of criteria to identify transects to be analyzed. (1) Only transects that contained the upwelling front and extended at least ±10 km from the front were used for analysis, so that acoustically detected fish biomass could be compared between offshore and inshore of the fronts. (2) Transects were required to contain a region of high biomass, defined as the NASC values exceeding 1 standard deviation (SD) from the mean which was estimated for each cruise (Table 1). By setting these thresholds, we excluded from the analysis transects with consistently low biomass in the entire transect. In order to compare transects having variable maximum values, NASC values were normalized by the maximum NASC value observed along each transect. The number of transects which met the above criteria were 5–8, depending on the cruises. (3) Distance between the normalized NASC and the upwelling front was calculated for at least 2 transect lines per cruise. Data from at least 2 transects, which met criteria (1) and (2), were binned into 10 km segments for each cruise. To avoid temporal changes in the locations of the upwelling fronts within the survey conducted over as long as 19 d, we estimated the longitudinal distance to the upwelling front identified on the same transect, that was separated by less than 9 h. The potential effect of choosing the upwelling front closest to shore would be minimal because we combined the data from multiple transects and binned them into 10 km segments, increasing the sample size. Statistical differences of the normalized NASC values between offshore and inshore of the upwelling front were tested using a Mann-Whitney *U*-test. Zooplankton distributions were examined for each cruise following the same criteria described above, using the 200 m isobaths as reference points. The number of transects which met the criteria (1) and (2) were 6–9, depending on the cruises.

Seasonal changes in fish distributions relative to the upwelling front, and zooplankton distributions relative to the 200 m isobath were examined. First, variability in the locations of the upwelling fronts was estimated by taking averages and SDs of the distance between the fronts and the 200 m isobaths for all the transects containing the front. Secondly, high biomass regions of fish and zooplankton (NASC > mean + 1 SD) were extracted. We used transects that contained high biomass regions regardless of their lengths, so that we had the minimum of 2 transects in the northern and southern zones, respectively, for comparison. Transects were required to include the upwelling fronts for fish and the 200 m isobaths for zooplankton, so that our analysis on their spatial distributions relative to each reference point was unbiased. The total number of transects which met these criteria was 8–13 for fish and 6–10 for zooplankton depending on the cruises. Means and SDs of the location of high biomass were examined for each cruise, corresponding to the cumulative alongshore wind stress measured off Newport for the northern zone and off Crescent City for the southern zone.

RESULTS

Upwelling characteristics

The upwelling season started earlier in the southern zone compared to the northern zone, with stronger wind stress towards the south. In 2000, the spring transition occurred 17 d earlier off Crescent City than off Newport. The June mesoscale survey corresponding to the early part of the cruise was conducted during upwelling favorable (southward) wind, while the rest of the survey corresponded to a period of northward wind events resulting in downwelling conditions (Fig. 3a,b). After this downwelling event, the winds were consistently upwelling favorable. Cumulative wind stress reached 0.4–0.8 N m^{-2} d during the June cruise and 2.6–3.2 N m^{-2} d during the August cruise off Newport, and 2.3–2.7 N m^{-2} d during June and 6.2–6.9 N m^{-2} d during August off Crescent City (Fig. 3c). In 2002, the spring transition occurred 28 d earlier off Crescent City than off Newport. Relatively consistent upwelling-favorable wind was observed during both June and August cruises (Fig. 3d,e). Cumulative wind stress was 2.1–2.7 N m^{-2} d during June and 3.7–4.2 N m^{-2} d during August off Newport, and 5.7–7.3 N m^{-2} d during June and 9.0–10.1 N m^{-2} d during August off Crescent City (Fig. 3f).

The spatial map of temperature at 5 m depth showed a narrow band of cold, saltier water along the coast during the June 2000 cruise, generally following the 200 m isobath throughout the study area (Fig. 4a; Barth et al. 2005). The exception was the penetration of warm, fresher surface waters (remnants of the Columbia River plume) onshore of the 200 m isobath at Heceta Bank. The position of the geopotential anomaly contour of 1.8 m^2 s^{-2}, indicating the location of the upwelling front, closely matched with the sharp change in temperature. Chlorophyll *a* concentrations were high at Heceta Bank, off Coos Bay, and south of Cape Blanco

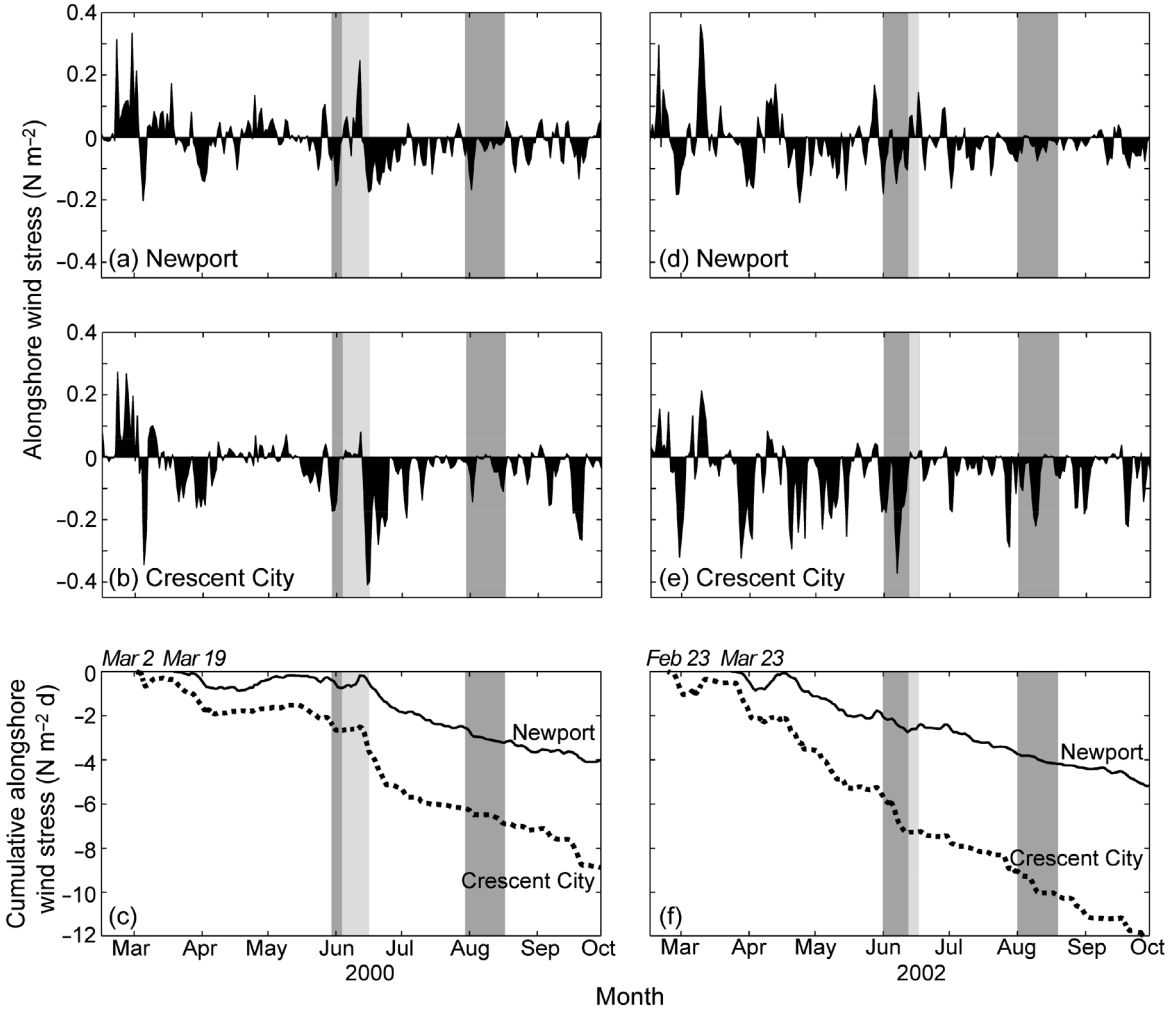

Fig. 3. (a,b,d,e) Alongshore wind stress and (c,f) cumulative alongshore wind stress measured at the NOAA buoys located off Newport and Crescent City. Negative values indicate southward (upwelling favorable) wind stress. Periods of field surveys during upwelling periods are shown by dark gray bars, while downwelling periods excluded from the analyses are shown by light gray bars. Dates in (c,f) indicate the spring transitions

(Fig. 4e). Upwelling features during June 2002 showed considerable along-shore variability (Fig. 4b). Upwelled waters were close to the shore in the northern zone, while there was a broadening of the upwelling region in the southern zone. High chlorophyll concentrations associated with the upwelling front were observed over Heceta Bank, off Cape Blanco, and farther offshore south of Cape Blanco (Fig. 4f). During August 2000, intensified upwelling characterized by colder and saltier surface waters compared to the conditions during June 2000 was observed along the coast (Fig. 4c; Barth et al. 2005). The upwelling region became broader over Heceta Bank, and there was a considerable warming of offshore waters. Local surface heating can account for the observed warmer surface temperatures. The upwelling front showed mesoscale variability which turned offshore off Cape Blanco (Fig. 4c) associated with relatively cold and saltier waters, representing a large anticyclonic meander. Chlorophyll *a* concentrations reaching 18.4 mg m^{-3} were observed at Heceta Bank, and some patches were associated with the shelf off Cape Blanco and farther south (Fig. 4g). The upwelling front moving offshore of Cape Blanco also carried chlorophyll-rich surface waters. During August 2002, intensified upwelling and increased mesoscale variability was also observed (Fig. 4d). Upwelling regions became broader along the coast, and there were discrete patches of high chlorophyll concentrations both offshore and inshore of the upwelling front (Fig. 4h). The separating upwelling front off Cape Blanco created an offshore eddy

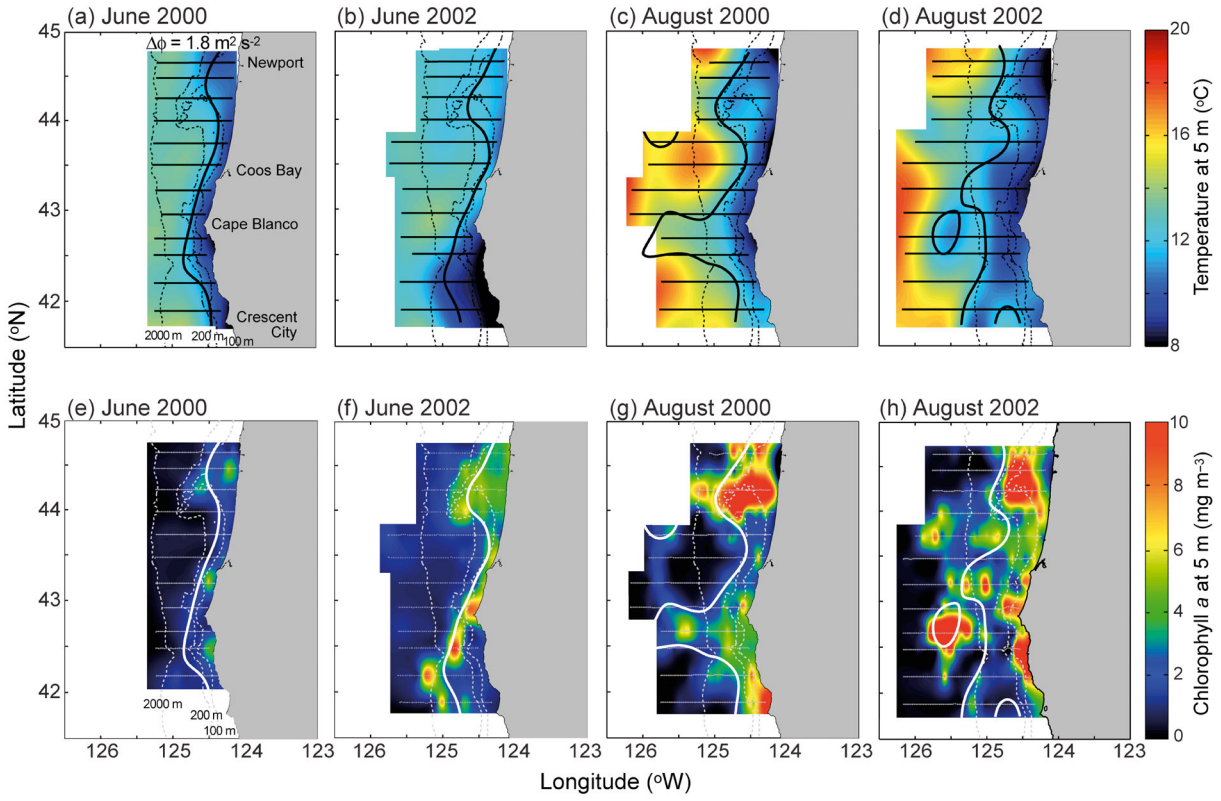

Fig. 4. (a–d) Temperature and (e–h) chlorophyll *a* concentrations at 5 m depth measured on the mesoscale transects (horizontal lines; both day and night). The contours of the upwelling fronts, defined as geopotential anomaly of 1.8 m^2 s^{-2}, are shown by thick solid lines. The 100, 200, and 2000 m isobaths are shown by thin, dotted lines. The southernmost transect during June 2000 cruise in (e) was excluded from analysis due to the malfunction of the fluorometer. Similar upwelling characteristics were apparent in the salinity data (not shown), with saltier water located inshore of the upwelling front along the coast

(42.8° N, 125.5° W) with low temperatures and high concentrations of chlorophyll.

Spatial distributions of planktivorous fish and their zooplankton prey

We observed seasonal variability of integrated acoustic scattering of fish. There was consistently low biomass throughout all transects during June 2000, high biomass with patchy distributions during June 2002 and August 2000, and a few high biomass regions during August 2002 (Table 1, Fig. 5a–d). During the June 2002 and August 2000 cruises, higher biomass was observed offshore than inshore of the upwelling front (Fig. 5b,c) with a clear boundary at the front (Fig. 6b,c). Normalized NASC values were significantly higher offshore than inshore of the front during June 2002 ($p < 0.01$) and August 2000 ($p < 0.05$). During June 2000 and August 2002, higher NASC values were observed both offshore and across the front, and a decrease in biomass occurred at 20–40 km inshore of the front (Fig. 6a,d). Thus, there was no significant difference in biomass between offshore and inshore of the front ($p = 0.06$ for June 2000, $p = 0.91$ for August 2002).

Trawl catches collected near the aggregations of acoustically detected fish were composed of a mixture of planktivorous fish. The catch during June 2002 was dominated by juvenile rockfishes (*Sebastes* spp.; SL = 29.0 ± 7.9 mm [mean ± SD]) comprising 90.1% of the mean areal density. The catch during August 2000 was dominated by jack mackerel *Trachurus symmetricus* (FL = 489.9 ± 31.3 mm) comprising 60.9% of the catch, followed by larval stages of Dover sole *Microstomus pacificus* and rex sole *Errex zachirus* (SL = 38.5 ± 14.7 mm) comprising 20.1%. Other catches included juvenile salmon, myctophids, juvenile Pacific sandlance *Ammodytes personatus*, blue shark *Prionace glauca*, juvenile and adult Pacific saury *Cololabis saira*, and larval northern anchovy *Engraulis mordax*. Since the trawls were conducted near the surface, fish inhabiting deeper depths were not targeted.

Integrated acoustic scattering of zooplankton showed consistently low biomass in most of the transects during June 2000, while there were patches

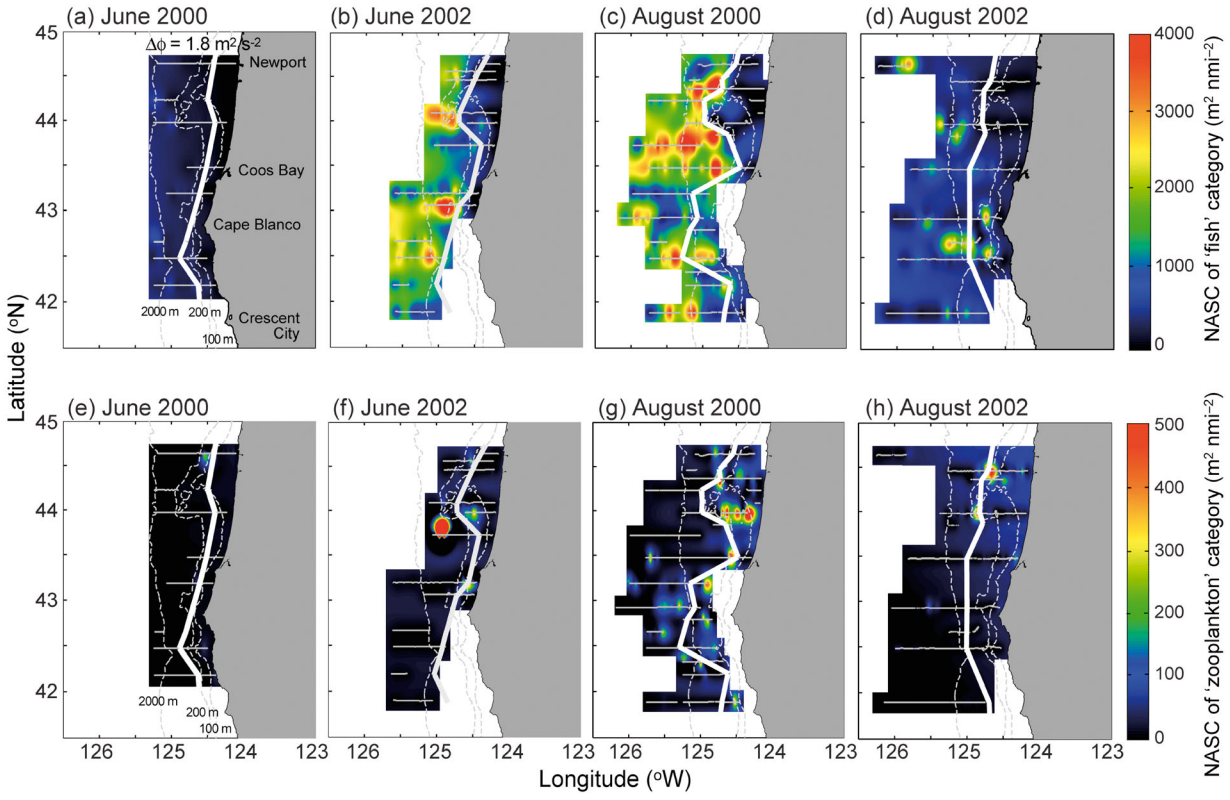

Fig. 5. Spatial distributions of daytime nautical area scattering coefficient (NASC) values of (a–d) fish and (e–h) zooplankton. White solid lines correspond to the location of the upwelling fronts, defined as geopotential anomaly of 1.8 $m^2 s^{-2}$, detected on the same transects used for the acoustic surveys. To avoid the effect of temporal changes in the upwelling front locations within the cruises, spatial smoothing of the front was not conducted. Horizontal lines are the transects, and dotted lines are the isobaths at 100, 200, and 2000 m

generally associated with the 200 m isobaths between 20 km offshore and 40 km inshore of the isobaths, or shallower depth during June 2002, August 2000, and August 2002 (Table 1, Fig. 5e–h). High biomass regions were located across the 200 m isobaths, with the majority of peaks located inshore for all cruises (Fig. 6e–h). Euphausiids (*Euphausia pacifica, Thysanoessa spinifera*) were the dominant taxa collected from daytime zooplankton scattering layers, constituting 54.5–100% of density. Pteropods (*Limacina* spp.) are strong acoustic targets and contribute high S_v values (Stanton et al. 1994), but were rare in our samples (<1%) collected within zooplankton scattering layers. The majority of acoustically detected zooplankton conducted diel vertical migration, because night NASC values of zooplankton at depth were only 4.2–28.8% of those during daytime.

We observed the shift of the upwelling front toward offshore as a function of cumulative alongshore wind stress (Fig. 7). In the northern zone, the upwelling front was located at 24.8 ± 17.0 km inshore of the 200 m isobath early in the upwelling season, moving to 10.4 ± 14.9 km offshore of the isobath later in the season. In the southern zone, where upwelling was stronger compared to the northern zone, the upwelling front moved from 3.9 ± 9.1 km offshore of the 200 m isobath to 24.1 ± 16.1 km offshore as upwelling intensified. The high biomass of planktivorous fish was mostly located offshore of the upwelling front, except during August 2002 when their distributions became wider covering both inshore and offshore sides of the front, while zooplankton were consistently located inshore or across the 200 m isobath. During the period of increased fish biomass, corresponding to June 2002 and August 2000 cruises, high biomass of planktivorous fish was located offshore of the upwelling front, while zooplankton were consistently located inshore or across the 200 m isobaths (Fig. 7).

DISCUSSION

We assessed the spatial variability of planktivorous fish and their dominant zooplankton prey associated with the seasonal and latitudinal variability of the up-

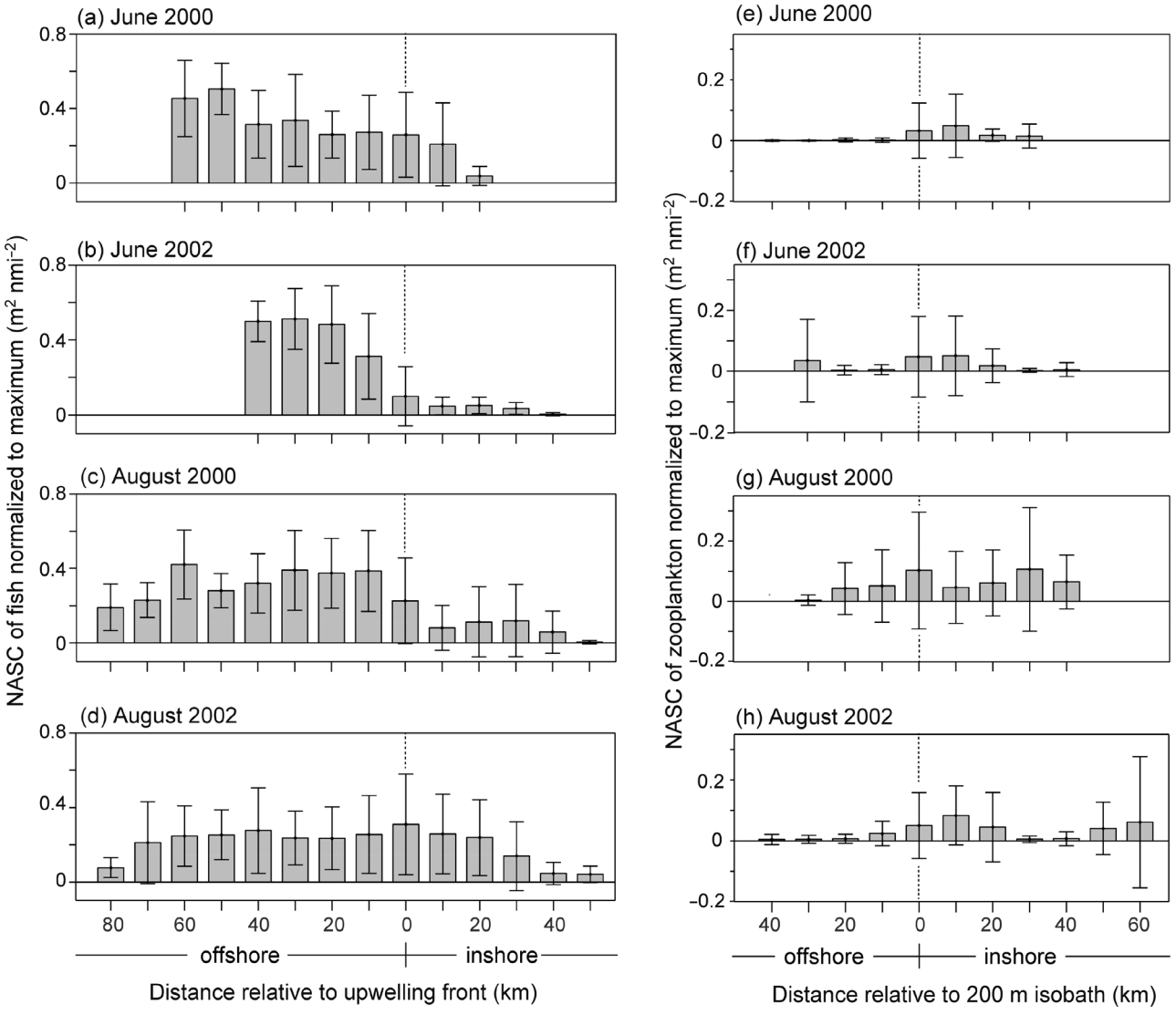

Fig. 6. Horizontal distributions of nautical area scattering coefficient (NASC) values of (a–d) fish relative to the upwelling front and (e–h) zooplankton relative to the 200 m isobath normalized to the maximum value of each transect. Bars show the average and errors bars show SD

welling fronts in the Northern California Current System. Acoustically observed fish biomass was higher offshore of the upwelling front than inshore, with statistically significant differences during the period of overall increased fish biomass corresponding to the June 2002 and August 2000 cruises. Trawl catches were dominated by planktivorous fish mostly composed of juvenile rockfishes and jack mackerel, both of which feed primarily on euphausiids (*Thysanoessa spinifera*, *Euphausia pacifica*) during summer (Brodeur et al. 1987, Miller & Brodeur 2007, Miller et al. 2010, Bosley et al. 2014). The high biomass of acoustically detected zooplankton, dominated by euphausiids, was generally associated with the 200 m isobath. Distributions of planktivorous fish offshore of the upwelling fronts corresponded to the warmer temperature, not to their zooplankton prey biomass, which was consistent with our hypothesis of physiological tolerance having significant impact on their distributions.

Persistent fish distributions offshore of the upwelling front suggest that the upwelling front acts as a shoreward boundary at the mesoscale. Because of the dynamic nature of upwelling systems coupled with co-varying water properties across the fronts, it is difficult to identify the mechanisms driving biological responses. Temperature has been considered as the most important factor determining geographical distributions of fish, because the metabolic rate of all ectothermic organisms is strongly dependent on temperature influencing their growth and reproduction

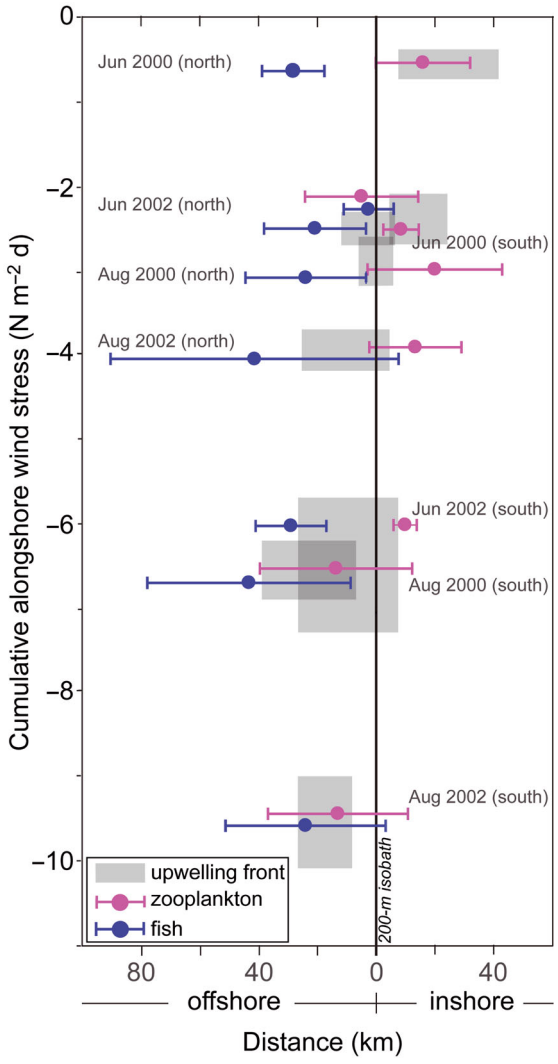

Fig. 7. Horizontal distributions of the upwelling fronts and high biomass of fish and zooplankton relative to the 200 m isobath as a function of cumulative alongshore wind stress. Upwelling fronts are shown in gray boxes whose height represents the survey period and width shows mean ± SD of the locations of the upwelling fronts. Circles show the mean, and error bars show the SD of fish and zooplankton distributions. Note that fish and zooplankton data are offset slightly for visual clarity

(Pörtner & Knust 2007, Pörtner & Farrell 2008, Sunday et al. 2011). In the California Current System, planktivorous fish distributions are tightly linked to ocean temperature (Lluch-Belda et al. 1992, Kaltenberg et al. 2010, Reese et al. 2011) which is consistent with our observations confining fish in the regions of warmer temperature. Seasonal appearance of fish schools dominated by northern anchovy, Pacific sardine, and whitebait smelt *Allosmerus elongatus* off Oregon occurred when sea surface temperature increased to ~11°C (Kaltenberg et al. 2010). Sardine and anchovy spawning distributions were linked to specific sea surface temperature: 13–25°C for sardines and 11.5–16.5°C for anchovies (Lluch-Belda et al. 1991).

Species-specific temperature ranges may explain seasonal shifts in fish distributions relative to the upwelling fronts. Among the planktivorous fish commonly observed in upwelling regions, jack mackerel and Pacific sardine *Sardinops sagax* tend to inhabit warmer waters than northern anchovy (Baxter 1966, Castillo et al. 1996, Checkley et al. 2000, Reiss et al. 2008). The shift in the transition point of fish biomass inshore of the front during the June 2000 and August 2002 cruises (Fig. 6a,d) may be due to the seasonal change in species composition toward those that prefer colder waters. Alternatively, life-stage specific preference in temperature range may cause the seasonal shifts in fish distributions. Early life stages have broader or narrower windows of thermal tolerance, depending on the species (Peck et al. 2013). We could not examine these hypotheses further, because we did not have trawl samples targeting the fish acoustic layers during all cruises. It is also possible that fish larger than those captured by the trawl were the primary constituents of the acoustically observed fish layers due to net avoidance behavior of fast-swimming organisms (Kaartvedt et al. 2012, Davison et al. 2015). Fish inhabiting waters close to the surface (<9 m depth) could not be detected in this study due to the blind zone of the ship-based acoustic surveys, potentially introducing a partial vertical mismatch between acoustic measurements and trawl sampling.

In addition to temperature, other factors may play a role in planktivorous fish distributions. In the Humboldt Current System, both temperature and salinity were considered as the important drivers of the distribution of sardine, anchovy, and jack mackerel (Castillo et al. 1996). Because temperature and salinity co-vary across the fronts, it is difficult to decouple their effects on fish distributions. Hypoxia is an increasing threat for coastal ecosystems, affecting the quantity and quality of habitat available to organisms (Breitburg et al. 2009). In the California Current system, anoxia in the water column is expanding (Chan et al. 2008), and the upper boundary of the oxygen minimum layer has shoaled by up to 90 m over the last 20 yr (Bograd et al. 2008). Fish are generally more vulnerable to low oxygen levels than zooplankton (Ekau et al. 2010). Thus, a decrease in dissolved oxygen associated with upwelling of hypoxic bottom waters may result in their avoidance of nearshore waters. However, dissolved oxygen concentration alone cannot explain physiological stress posed by hypoxia because metabolic rates of animals are tem-

perature dependent (He et al. 2015). Physiological stress due to inhabiting decreased dissolved oxygen waters may be mitigated by lower metabolic rates in colder water (Pörtner & Knust 2007, Deutsch et al. 2015, Sato et al. 2016), associated with upwelling. Long-term, high-resolution measurements of multiple environmental characteristics would be needed in the future to decouple the co-varying factors and determine the driving mechanism of planktivorous fish distributions in the dynamic upwelling systems.

Aggregations of euphausiids along the shelf break have been previously observed. In the Northern California Current System, euphausiids aggregate inshore of Heceta Bank and off Cape Blanco between the 200 and 800 m isobaths (Ressler et al. 2005, Swartzman et al. 2005). Complex interactions of the poleward undercurrent, bottom topography, and diel vertical migration behavior have been suggested to create and maintain euphausiid aggregations in upwelling regions (Mackas et al. 1997, Ressler et al. 2005, Swartzman et al. 2005), which may also explain the mismatch between the acoustic distribution of euphausiids and high chlorophyll concentrations. Locations of euphausiid aggregations and their daytime depth observed in this study generally agreed with the previous studies, with euphausiids aggregating around the 200 m isobaths. Even if euphausiids concentrate over deeper isobaths (Swartzman et al. 2005), beyond the range of the ship-based acoustics used in this study, our conclusion that euphausiids aggregate near an upper-slope isobath rather than the position of the upwelling front likely holds. This is because the 200 and 800 m isobaths in this area are parallel and close together (approximately <23 km apart; Pierce et al. 2000).

Recruitment success of higher trophic levels is highly dependent on temporal (Hjort 1914, Cushing 1974, 1990) and spatial (Chick & Van Den Avyle 1999, Durant et al. 2007) synchronization with their prey. Since euphausiids are one of the primary prey for the planktivorous fish observed in our study site during summer (Miller et al. 2010), spatial overlap with their zooplankton prey is critical. Differences in reference points controlling the distributions of planktivorous fish and zooplankton suggest that shifts in their relative positions may play an important role in predator–prey interactions. The offshore movement of the upwelling front away from the 200 m isobath as the upwelling season progressed suggests a decrease in horizontal overlap between planktivorous fish and euphausiids. Because Heceta Bank extends offshore, the upwelling front was located inshore of the 200 m isobath early in the upwelling season, potentially causing greater overlap between planktivorous fish and their zooplankton prey. During the period of fully developed upwelling, the front closely matched with the 200 m isobath creating a spatial gap between fish and zooplankton. Separation of the coastal upwelling jet also occurs near Cape Blanco, where the jet often turns westward or northward due to the subsequent anticyclonic meandering (Barth et al. 2000, 2005). Thus, aggregations of euphausiids on the shelf and slope off Cape Blanco (Ressler et al. 2005, Swartzman et al. 2005) may only be seasonally or intermittently accessible to planktivorous fish. In addition to horizontal overlap, feeding success of fish requires vertical overlap with their zooplankton prey. Here, we explicitly assume that the vertical overlap between planktivorous fish and euphausiids occurs at night when euphausiids migrate to shallower depths. This assumption, however, may not apply due to depth-dependent offshore transport within the Ekman layer (Peterson 1998) whereby subtle changes in vertical positioning of zooplankton can cause retention or dispersal. To separate fish from zooplankton at night when they are likely to co-locate, high-resolution sampling will be required.

Seasonal variability in accessibility to their prey can greatly impact recruitment success of fish populations. Commonly observed planktivorous fish off Oregon, such as jack mackerel and Pacific sardine, undergo extensive northward feeding migrations during summer (Brodeur et al. 2005, Kaltenberg & Benoit-Bird 2009, Litz et al. 2014). Pacific sardines also spawn in offshore regions of the Northern California Current System in summer (Emmett et al. 2005). Our observations of high fish biomass during June 2002 and August 2000 cruises likely captured this seasonal feeding and/or spawning migration, while June 2000 and August 2002 cruises were likely before and after the migration as indicated by the very low acoustic scattering values (Table 1). There is significant latitudinal variability in southward wind forcing during summer, increasing wind strength in the south and resulting in longer upwelling periods in southern latitudes (Huyer 1983, Bograd et al. 2009). Consequently, the time window of increased predator–prey overlap could be shorter in the south. If access to their zooplankton prey is seasonally limited, there may be a critical time period for seasonally migrating pelagic fish to appear in the Northern California Current System.

Spatial mismatch between planktivorous fish and their zooplankton prey may be accelerated in the future due to climate change. Although there are latitudinal and seasonal dependencies in projected upwelling-favorable wind intensity within the Cali-

fornia Current System (Rykaczewski et al. 2015), intensification of upwelling-favorable winds due to global warming is anticipated in the Northern California Current System during summer (Bakun 1990, Sydeman et al. 2014, García-Reyes et al. 2015, Rykaczewski et al. 2015). Wind intensification could benefit marine ecosystems by increasing nutrient input into euphotic zones if primary production is nutrient-limited. Such changes, however, do not necessarily translate into increase in productivity across food webs. With strongly enhanced upwelling, the upwelling front would move farther offshore in the future (Bakun et al. 2015). Planktivorous fish that remain offshore of the front consequently increase the spatial gap with their zooplankton prey. Based on the latitudinal difference in predator–prey overlap, the degree of this decoupling will likely be greater in the southern zone than in the northern zone. Any decrease in the frequency of spatial overlap with their dominant prey could adversely impact recruitment success of commercially important fish species in the Northern California Current System.

The role of an upwelling front as a boundary for planktivorous fish distributions is an important mechanism controlling predator–prey overlap. The spatial mismatch between planktivorous fish and their zooplankton prey is likely alleviated during relaxation periods due to the onshore movement of the fronts. The short timescale of relaxation events in our study site, approximately 8 d (Austin & Barth 2002), suggests the potential for frequent spatial overlap between predators and prey with the degree of the overlap depending on the distance of the onshore movement of the fronts during relaxation as well as the response time of planktivorous fish. Based on the assumed role of fronts as bio-aggregators across the food web providing foraging locations, distance to the upwelling front has been considered as one of the key factors controlling spatial distributions of higher trophic level predators including seabirds and marine mammals (Ainley et al. 2005, 2009, Tynan et al. 2005). However, our results of the upwelling front acting as a shoreward boundary suggest that prey availability would be significantly different between inshore and offshore of the front. Instead of the traditional view of fronts as bio-aggregators which ignores the directionality (i.e. inshore vs. offshore), the location of piscivorous species relative to the front has significant impact on their prey availability. The boundary effect of the fronts on the distributions of mid-trophic level organisms suggests its important role on predator–prey interactions and energy transfer through coastal food webs.

Acknowledgements. We thank the crews of the RVs 'Wecoma', 'Thomas G. Thompson', 'Roger Revelle', and 'New Horizon', and the FVs 'Sea Eagle' and 'Frosti', and all the people involved in the Northeast Pacific GLOBEC project for collecting the interdisciplinary field data. We especially thank the Oregon State University Marine Technicians, in particular M. Willis, for helping us safely tow the bioacoustics sled while SeaSoaring along the transects during day and night, including dodging the occasional surface floats of crab pots. J. Fisher provided zooplankton MOCNESS data, and P. Nealson at Hydroacoustics Technology, Inc., assisted with reviewing calibration values and transducer positioning on the towed body. We thank 3 anonymous reviewers for their comments to improve the manuscript. The GLOBEC project was supported by a National Science Foundation Grant (OCE-0001035). M.S. was supported by the W. M. Keck Foundation grant to J.A.B., K.J.B., and G. Hollinger.

LITERATURE CITED

Ainley DG, Spear LB, Tynan CT, Barth JA, Pierce SD, Ford RG, Cowles TJ (2005) Physical and biological variables affecting seabird distributions during the upwelling season of the northern California Current. Deep-Sea Res II 52:123–143

Ainley DG, Dugger KD, Ford RG, Pierce SD and others (2009) Association of predators and prey at frontal features in the California Current: competition, facilitation, and co-occurrence. Mar Ecol Prog Ser 389:271–294

Austin JA, Barth JA (2002) Variation in the position of the upwelling front on the Oregon shelf. J Geophys Res Oceans 107:3180

Bakun A (1990) Global climate change and intensification of coastal ocean upwelling. Science 247:198–201

Bakun A (1996) Patterns in the ocean: ocean processes and marine population dynamics. California Sea Grant, in cooperation with Centro de Investigaciones Biologicas del Noroeste, La Paz

Bakun A, Black BA, Bograd SJ, Garcia-Reyes M, Miller AJ, Rykaczewski RR, Sydeman WJ (2015) Anticipated effects of climate change on coastal upwelling ecosystems. Curr Clim Change Rep 1:85–93

Barth JA, Pierce SD, Smith RL (2000) A separating coastal upwelling jet at Cape Blanco, Oregon and its connection to the California Current System. Deep-Sea Res II 47: 783–810

Barth JA, Pierce SD, Cowles TJ (2005) Mesoscale structure and its seasonal evolution in the northern California Current System. Deep-Sea Res II 52:5–28

Batchelder HP, Barth JA, Kosro PM, Strub PT and others (2002) The GLOBEC Northeast Pacific California Current System Program. Oceanography 15:36–47

Baxter JL (1966) Summary of biological information on the northern anchovy *Engraulis mordax* Girard. Calif Coop Ocean Fish Invest Rep 11:110–116

Belkin IM, Cornillon PC, Sherman K (2009) Fronts in large marine ecosystems. Prog Oceanogr 81:223–236

Bograd SJ, Castro CG, Di Lorenzo E, Palacios DM, Bailey H, Gilly W, Chavez FP (2008) Oxygen declines and the shoaling of the hypoxic boundary in the California Current. Geophys Res Lett 35:L12607

Bograd SJ, Schroeder I, Sarkar N, Qiu X, Sydeman WJ, Schwing FB (2009) Phenology of coastal upwelling in the California Current. Geophys Res Lett 36:L01602

Bosley KL, Miller TW, Brodeur RD, Bosley KM, Van Gaest A, Elz A (2014) Feeding ecology of juvenile rockfishes off

Oregon and Washington based on stomach content and stable isotope analyses. Mar Biol 161:2381–2393

Bost CA, Cotté C, Bailleul F, Cherel Y and others (2009) The importance of oceanographic fronts to marine birds and mammals of the southern oceans. J Mar Syst 78:363–376

Breitburg DL, Hondorp DW, Davias LA, Diaz RJ (2009) Hypoxia, nitrogen, and fisheries: integrating effects across local and global landscapes. Annu Rev Mar Sci 1:329–349

Brodeur RD, Lorz HV, Pearcy WG (1987) Food habits and dietary variability of pelagic nekton off Oregon and Washington, 1979-1984. NOAA Tech Rep NMFS 57, US Department of Commerce, Springfield, VA

Brodeur RD, Fisher JP, Teel DJ, Emmett RL, Casillas E, Miller TW (2004) Juvenile salmonid distribution, growth, condition, origin, and environmental and species associations in the Northern California Current. Fish Bull 102: 24–46

Brodeur RD, Fisher JP, Emmett RL, Morgan CA, Casillas E (2005) Species composition and community structure of pelagic nekton off Oregon and Washington under variable oceanographic conditions. Mar Ecol Prog Ser 298: 41–57

Castelao RM, Barth JA, Mavor TP (2005) Flow-topography interactions in the northern California Current System observed from geostationary satellite data. Geophys Res Lett 32:L24612

Castillo J, Barbieri MA, Gonzalez A (1996) Relationships between sea surface temperature, salinity, and pelagic fish distribution off northern Chile. ICES J Mar Sci 53: 139–146

Chan F, Barth JA, Lubchenco J, Kirincich A, Weeks H, Peterson WT, Menge BA (2008) Emergence of anoxia in the California Current large marine ecosystem. Science 319: 920

Checkley DM Jr, Dotson RC, Griffith DA (2000) Continuous, underway sampling of eggs of Pacific sardine (*Sardinops sagax*) and northern anchovy (*Engraulis mordax*) in spring 1996 and 1997 off southern and central California. Deep-Sea Res II 47:1139–1155

Chick JH, Van Den Avyle MJ (1999) Zooplankton variability and larval striped bass foraging: evaluating potential match/mismatch regulation. Ecol Appl 9:320–334

Cushing DH (1974) The natural regulation of fish populations. In: Harden-Jones FR (ed) Sea fisheries research. Elek Science, London, p 399–412

Cushing DH (1990) Plankton production and year-class strength in fish populations: an update of the match/mismatch hypothesis. Adv Mar Biol 26:249–293

Davison PC, Koslow JA, Kloser RJ (2015) Acoustic biomass estimation of mesopelagic fish: backscattering from individuals, populations, and communities. ICES J Mar Sci 72:1413–1424

De Robertis A, Higginbottom I (2007) A post-processing technique to estimate the signal-to-noise ratio and remove echosounder background noise. ICES J Mar Sci 64: 1282–1291

Deutsch C, Ferrel A, Seibel B, Pörtner HO, Huey RB (2015) Climate change tightens a metabolic constraint on marine habitats. Science 348:1132–1135

Durant JM, Hjermann DØ, Ottersen G, Stenseth NC (2007) Climate and the match or mismatch between predator requirements and resource availability. Clim Res 33: 271–283

Ekau W, Auel H, Pörtner HO, Gilbert D (2010) Impacts of hypoxia on the structure and processes in pelagic communities (zooplankton, macro-invertebrates and fish). Biogeosciences 7:1669–1699

Emmett RL, Brodeur RD, Miller TW, Pool SS, Bentley PJ, Krutzikowsky GK, McCrae J (2005) Pacific sardine (*Sardinops sagax*) abundance, distribution and ecological relationships in the Pacific Northwest. Calif Coop Ocean Fish Invest Rep 46:122–143

Feinberg LR, Peterson WT (2003) Variability in duration and intensity of euphausiid spawning off central Oregon, 1996–2001. Prog Oceanogr 57:363–379

Franks PJ (1992a) Phytoplankton blooms at fronts: patterns, scales, and physical forcing mechanisms. Rev Aquat Sci 6:121–137

Franks PJS (1992b) Sink or swim: accumulation of biomass at fronts. Mar Ecol Prog Ser 82:1–12

García-Reyes M, Sydeman WJ, Schoeman DS, Rykaczewski RR, Black BA, Smit AJ, Bograd SJ (2015) Under pressure: climate change, upwelling, and eastern boundary upwelling ecosystems. Front Mar Sci 2:109

Genin A, Jaffe JS, Reef R, Richter C, Franks PJ (2005) Swimming against the flow: a mechanism of zooplankton aggregation. Science 308:860–862

Haury LR, McGowan JA, Wiebe PH (1978) Patterns and processes in the time-space scales of plankton distributions. In: Steele JH (ed) Spatial pattern in plankton communities. Springer US, Boston, MA, p 277–327

He W, Cao ZD, Fu SJ (2015) Effect of temperature on hypoxia tolerance and its underlying biochemical mechanism in two juvenile cyprinids exhibiting distinct hypoxia sensitivities. Comp Biochem Physiol A Mol Integr Physiol 187: 232–241

Hjort J (1914) Fluctuations in the great fisheries of northern Europe viewed in the light of biological research. Rapp P-V Reun (Dan) 20:1–228

Huyer A (1983) Coastal upwelling in the California Current system. Prog Oceanogr 12:259–284

Huyer A, Sobey EJC, Smith RL (1979) The spring transition in currents over the Oregon continental shelf. J Geophys Res 84:6995–7011

Joyce TM (1983) Varieties of ocean fronts. In: Stern ME, Mellor FK (eds) Baroclinic instability and ocean fronts. Technical Report No. 83-41. Woods Hole Oceanographic Institution, Woods Hole, MA

Kaartvedt S, Staby A, Aksnes DL (2012) Efficient trawl avoidance by mesopelagic fishes causes large underestimation of their biomass. Mar Ecol Prog Ser 456:1–6

Kaltenberg AM, Benoit-Bird KJ (2009) Diel behavior of sardine and anchovy schools in the California Current System. Mar Ecol Prog Ser 394:247–262

Kaltenberg AM, Emmett RL, Benoit-Bird KJ (2010) Timing of forage fish seasonal appearance in the Columbia River plume and link to ocean conditions. Mar Ecol Prog Ser 419:171–184

Kang M, Furusawa M, Miyashita K (2002) Effective and accurate use of difference in mean volume backscattering strength to identify fish and plankton. ICES J Mar Sci 59:794–804

Lamb J, Peterson W (2005) Ecological zonation of zooplankton in the COAST study region off central Oregon in June and August 2001 with consideration of retention mechanisms. J Geophys Res 110:C10S15

Lara-Lopez AL, Davison P, Koslow JA (2012) Abundance and community composition of micronekton across a front off Southern California. J Plankton Res 34:828–848

Large WG, Pond S (1981) Open ocean momentum flux measurements in moderate to strong winds. J Phys Oceanogr 11:324–336

Le Fèvre J (1987) Aspects of the biology of frontal systems. Adv Mar Biol 23:163–299

Litz MNC, Emmett RL, Bentley PJ, Claiborne AM, Barceló C (2014) Biotic and abiotic factors influencing forage fish and pelagic nekton community in the Columbia River plume (USA) throughout the upwelling season 1999–2009. ICES J Mar Sci 71:5–18

Lluch-Belda D, Lluch-Cota DB, Hernandez-Vazquez S, Salinas-Zavala CA, Schwartzlose RA (1991) Sardine and anchovy spawning as related to temperature and upwelling in the California current system. CalCOFI Rep 32:105–111

Lluch-Belda D, Schwartzlose RA, Serra R, Parrish R, Kawasaki T, Hedgecock D, Crawford RJ (1992) Sardine and anchovy regime fluctuations of abundance in four regions of the world oceans: a workshop report. Fish Oceanogr 1: 339–347

Logerwell EA, Smith PE (2001) Mesoscale eddies and survival of late stage Pacific sardine (*Sardinops sagax*) larvae. Fish Oceanogr 10:13–25

Mackas DL, Kieser R, Saunders M, Yelland DR, Brown RM, Moore DF (1997) Aggregation of euphausiids and Pacific hake (*Merluccius productus*) along the outer continental shelf off Vancouver Island. Can J Fish Aquat Sci 54: 2080–2096

McClatchie S, Cowen R, Nieto K, Greer A and others (2012) Resolution of fine biological structure including small narcomedusae across a front in the Southern California Bight. J Geophys Res Oceans 117:C04020

Miller TW, Brodeur RD (2007) Diets of and trophic relationships among dominant marine nekton within the northern California Current ecosystem. Fish Bull 105:548–559

Miller TW, Brodeur RD, Rau G, Omori K (2010) Prey dominance shapes trophic structure of the northern California Current pelagic food web: evidence from stable isotopes and diet analysis. Mar Ecol Prog Ser 420:15–26

Nishimoto MM, Washburn L (2002) Patterns of coastal eddy circulation and abundance of pelagic juvenile fish in the Santa Barbara Channel, California, USA. Mar Ecol Prog Ser 241:183–199

Peck MA, Reglero P, Takahashi M, Catalán IA (2013) Life cycle ecophysiology of small pelagic fish and climate-driven changes in populations. Prog Oceanogr 116:220–245

Peterson W (1998) Life cycle strategies of copepods in coastal upwelling zones. J Mar Syst 15:313–326

Pierce SD, Smith RL, Kosro PM, Barth JA, Wilson CD (2000) Continuity of the poleward undercurrent along the eastern boundary of the mid-latitude north Pacific. Deep-Sea Res II 47:811–829

Pörtner HO, Farrell AP (2008) Physiology and climate change. Science 322:690–692

Pörtner HO, Knust R (2007) Climate change affects marine fishes through the oxygen limitation of thermal tolerance. Science 315:95–97

Reese DC, Brodeur RD (2006) Identifying and characterizing biological hotspots in the northern California Current. Deep-Sea Res II 53:291–314

Reese DC, O'Malley RT, Brodeur RD, Churnside JH (2011) Epipelagic fish distributions in relation to thermal fronts in a coastal upwelling system using high-resolution remote-sensing techniques. ICES J Mar Sci 68:1865–1874

Reiss CS, Checkley DM, Bograd SJ (2008) Remotely sensed spawning habitat of Pacific sardine (*Sardinops sagax*) and Northern anchovy (*Engraulis mordax*) within the California Current. Fish Oceanogr 17:126–136

Ressler PH, Brodeur RD, Peterson WT, Pierce SD, Vance PM, Røstad A, Barth JA (2005) The spatial distribution of euphausiid aggregations in the Northern California Current during August 2000. Deep-Sea Res II 52:89–108

Rykaczewski RR, Dunne JP, Sydeman WJ, García-Reyes M, Black BA, Bograd SJ (2015) Poleward displacement of coastal upwelling-favorable winds in the ocean's eastern boundary currents through the 21st century. Geophys Res Lett 42:6424–6431

Sabarros PS, Ménard F, Lévénez JJ, Tew-Kai E, Ternon JF (2009) Mesoscale eddies influence distribution and aggregation patterns of micronekton in the Mozambique Channel. Mar Ecol Prog Ser 395:101–107

Sato M, Horne JK, Parker-Stetter SL, Keister JE (2015) Acoustic classification of coexisting taxa in a coastal ecosystem. Fish Res 172:130–136

Sato M, Horne JK, Parker-Stetter SL, Essington TE and others (2016) Impacts of moderate hypoxia on fish and zooplankton prey distributions in a coastal fjord. Mar Ecol Prog Ser 560:57–72

Seki MP, Polovina JJ, Kobayashi DR, Bidigare RR, Mitchum GT (2002) An oceanographic characterization of swordfish (*Xiphias gladius*) longline fishing grounds in the springtime subtropical North Pacific. Fish Oceanogr 11:251–266

Stanton TK, Wiebe PH, Chu D, Benfield MC, Scanlon L, Martin L, Eastwood RL (1994) On acoustic estimates of zooplankton biomass. ICES J Mar Sci 51:505–512

Sunday JM, Bates AE, Dulvy NK (2011) Global analysis of thermal tolerance and latitude in ectotherms. Proc R Soc B 278:1823–1830

Swartzman G, Hickey B, Kosro PM, Wilson C (2005) Poleward and equatorward currents in the Pacific Eastern Boundary Current in summer 1995 and 1998 and their relationship to the distribution of euphausiids. Deep-Sea Res II 52:73–88

Sydeman WJ, García-Reyes M, Schoeman DS, Rykaczewski RR, Thompson SA, Black BA, Bograd SJ (2014) Climate change and wind intensification in coastal upwelling ecosystems. Science 345:77–80

Tittensor DP, Mora C, Jetz W, Lotze HK, Ricard D, Berghe EV, Worm B (2010) Global patterns and predictors of marine biodiversity across taxa. Nature 466: 1098–1101

Traganza ED, Redalije DG, Garwood RW (1987) Chemical flux, mixed layer entrainment and phytoplankton blooms at upwelling fronts in the California coastal zone. Cont Shelf Res 7:89–105

Tynan CT, Ainley DG, Barth JA, Cowles TJ, Pierce SD, Spear LB (2005) Cetacean distributions relative to ocean processes in the northern California Current System. Deep-Sea Res II 52:145–167

Venegas RM, Strub PT, Beier E, Letelier R and others (2008) Satellite-derived variability in chlorophyll, wind stress, sea surface height, and temperature in the northern California Current System. J Geophys Res Oceans 113: C03015

Wiebe PH, Morton AW, Bradley AM, Backus RH and others (1985) New development in the MOCNESS, an apparatus for sampling zooplankton and micronekton. Mar Biol 87:313–323

Worm B, Sandow M, Oschlies A, Lotze HK, Myers RA (2005) Global patterns of predator diversity in the open oceans. Science 309:1365–1369

Yoder JA, Ackleson SG, Barber RT, Flament P, Balch WM (1994) A line in the sea. Nature 371:689–692

Young JW, Bradford R, Lamb TD, Clementson LA, Kloser R, Galea H (2001) Yellowfin tuna (*Thunnus albacares*) aggregations along the shelf break off south-eastern Australia: links between inshore and offshore processes. Mar Freshw Res 52:463–474

Appendix. Vertical separation of 'fish' and 'zooplankton' categories

Daytime survey data showed that both 'fish' and 'zooplankton' categories were vertically stratified into 2 depth zones: one in the upper water column (≤100 m depth and shallower than 60 m above the bottom), and one in the deeper water column or associated with the bottom (>100 m depth or within 60 m of the bottom; Fig. A1). To examine the effect of the upwelling front on spatial distributions of pelagic organisms, we focused on daytime 'fish' at shallower depths. Effects of near-surface frontal features on fish located at depth or associated with the bottom were less likely. We also excluded night-time 'fish' at shallower depths from the analysis because diel vertical migration of near-bottom fish toward shallower depths would complicate the interpretation of the surface pelagic fish distribution relative to the upwelling fronts. For the 'zooplankton' category, we focused on those observed at depth during daytime which are likely adult and juvenile euphausiids (Feinberg & Peterson 2003, Lamb & Peterson 2005). Zooplankton at shallower depths during day and night surveys were excluded from the analysis because zooplankton scattering layers could not be quantitatively characterized when they were co-located with fish due to low sampling resolution.

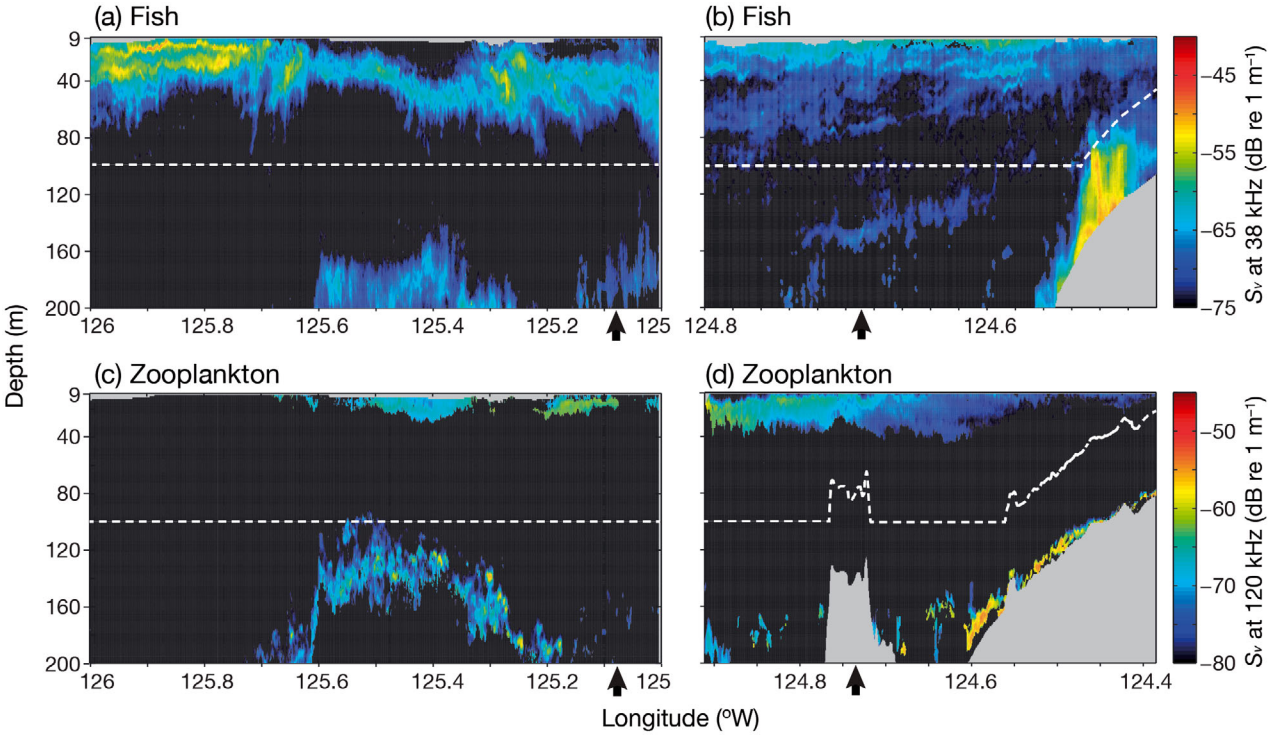

Fig. A1. Example echograms of volume backscattering strength (S_v) of vertically segregated (a,b) 'fish' and (c,d) 'zooplankton' categories during daytime in deep water and near the bottom. Dashed lines show a combination of 100 m depth and 60 m from the bottom used as threshold depths to separate 2 depth zones. Arrows indicate the locations of upwelling fronts. S_v data were from different survey lines: (a,c) along 43.0° N during August 2000, (b) along 41.9° N during August 2002 (not used in Fig. 5d), and (d) 44.7° N during August 2000 (not used in Fig. 5g)

Editorial responsibility: Kenneth Sherman, Narragansett, Rhode Island, USA

Submitted: August 15, 2017; Accepted: March 7, 2018
Proofs received from author(s): April 28, 2018